Available online at www.sciencedirect.com

SciVerse ScienceDirect

Energy Procedia 34 (2013) 791 – 800

Energy Procedia

10th Eco-Energy and Materials Science and Engineering

(EMSES2012)

Structural Characteristics and Dielectric Properties of $La_{1-x}Co_xFeO_3$ and $LaFe_{1-x}Co_xO_3$ Synthesized via Metal Organic Complexes

Wankassama Haron[a], Thammanoon Thaweechai[a], Worawat Wattanathana[a], Apirat Laobuthee[b], Hathaikarn Manaspiya[c], Chatchai Veranitisagul[d], Nattamon Koonsaeng[a]*

[a]*Department of Chemistry, Faculty of Science, Kasetsart University, Chatuchak, Bangkok, Thailand 10900*
[b]*Department of Materials Engineering, Faculty of Engineering, Kasetsart University, Bangkok 10900, Thailand*
[c]*The Petroleum and Petrochemical College, Chulalongkorn University, Phayathai, Bangkok, Thailand 10330*
[d]*Department of Material and Metallurgical Engineering, Faculty of Engineering, Rajamangala University of Technology Thanyaburi, Klong 6, Thanyaburi, Pathumthani 12110*

Abstract

$La_{1-x}Co_xFeO_3$ and $LaFe_{1-x}Co_xO_3$ perovskite-type oxides with $0.1 \le x \le 0.3$ are prepared by thermal decomposition of the metal organic complexes, using triethanolamine ($N(CH_2CH_2OH)_3$) as ligand and $La(NO_3)_3.6H_2O$ and $Fe(NO_3)_2.9H_2O$ as starting materials. $CoCl_2.6H_2O$ is used as the dopant. The obtained products calcined at 850°C for 2 h were characterized by XRD, FTIR, BET and SEM and their dielectric properties were investigated. It was found that all the as-prepared samples crystallized in orthorhombic structure of $LaFeO_3$ perovskite and exhibit conducting behavior. It suggests that the substituted Co(II) and oxygen deficiency play an important role in the ionic conductivity of these materials.

Selection and peer-review under responsibility of COE of Sustainalble Energy System, Rajamangala University of Technology Thanyaburi (RMUTT)

Keywords: Co(II)-doped $LaFeO_3$; dielectric property; $LaFeO_3$; metal-organic complexes

* Corresponding author. Tel.:+662-5625555 Ext.2189
E-mail address: fscinmk@ku.ac.th

Selection and peer-review under responsibility of COE of Sustainalble Energy System, Rajamangala University of Technology Thanyaburi (RMUTT)
doi:10.1016/j.egypro.2013.06.815

1. Introduction

Recently, substitution effects of various impurity ions into the A and B sites of perovskite oxide with chemical formula ABO_3 are scientifically attractive. Particularly, $LaFeO_3$-based oxides have been received much attention since they have potential as candidate materials for various applications in advanced technologies, such as, cathode materials in solid oxide fuel cells [1-3], catalysts [4], chemical sensors [5-8] and magnetic materials [9] etc. The preparation of $LaFeO_3$ and the related compounds have been achieved by many processes, including solid-solid reaction, co-precipitation, sol-gel, decomposition of cyanide and citrate methods [10-14].

According to our previous work, the $MgAl_2O_4$ and $NiAl_2O_4$ spinels including the $LaAlO_3$ perovskite are sucessfully prepared via decomposition of metal organic complexes consisting TEA as a ligand. This preparation method offers many advantages such as simple, low cost, exhibiting high purity and homogeneity products. In addition, the metal ion doped ceramic powders can be easily prepared by adding the amount of dopant into the reaction of complexing process. In this work, $La_{1-x}Co_xFeO_3$ and $LaFe_{1-x}Co_xO_3$ with $0.1 \leq x \leq 0.3$ are prepared by thermal decomposition of La-Fe-TEA complexes and the effects of partially metal ions doped to replace La(III) and Fe(III) at the A and B site of $LaFeO_3$ structure were characterized. Because dielectric properties of this type of compounds have rarely been studied so far [15], their dielectric properties are measured as a function of frequencies, at the ambient temperature. Dielectric constant and dielectric loss as the influence of Co(II) concentrations substituted at A or B site of $LaFeO_3$ based perovskite are also investigated.

2. Experimental

2.1. Materials

Lanthanum(III) nitrate hexahydrate ($La(NO_3)_3.6H_2O$) was purchased from Fisher Scientific. Iron(III) nitrate nonahydrate ($Fe(NO_3)_3.9H_2O$), Cobalt(II) chloride ($CoCl_2.6H_2O$), Triethanolamine (TEA, $N(CH_2CH_2OH)_3$) and Ethylene glycol (EG, $HOCH_2CH_2OH$) were purchased from Ajax Finechem. All reagents were used as received.

2.2. Methods

The synthesis process of $LaFeO_3$ and Co(II)-doped $LaFeO_3$ from the metal-organic complexes is illustrated in Figure 1.

The precursor, metal-organic complexes of $LaFeO_3$ (LFO) was prepared by the chemical reaction of $La(NO_3)_3.6H_2O$, $Fe(NO_3)_3.9H_2O$ and TEA with the 1 : 1 : 3 mole ratio of La(III) : Fe(III) : TEA in ethylene glycol (EG) solvent. The reaction mixture was distilled at 190°C for 6 h with continuous stirring. Distillation was carried out until nearly the 2/3 of EG had been evaporated. The complex was separated by filtration, washed twice with ethanol and dried at 80 ºC. The as-prepared metal-organic complex was characterized by TGA (761 Connecticut 06859 Perkin Elmer, heating rate of 10°C/min over 50°C to 1000°C temperature range).

Similarly, to obtain the Co(II) doped precursors of $La_{1-x}Co_xFeO_3$ (LCFO) and $LaFe_{1-x}Co_xO_3$ (LFCO) with x = 0.1, 0.2 and 0.3, the stoichiometric molar quantities of Co(II) : La(III) and Co(II) : Fe(III) as the ratio of 0.1 : 0.9, 0.2 : 0.8 and 0.3 : 0.7 were added.

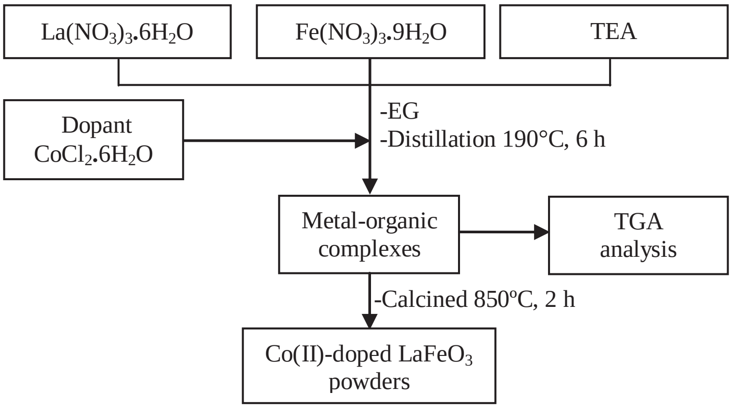

Fig. 1. Flow chart for Synthesis of $LaFeO_3$ and Co(II)-doped $LaFeO_3$ via Metal-organic Complexes

All metal-organic complexes were converted to ceramic powder by calcination under static air at 850°C for 2 h. The powder products were characterized by XRD, using CuK_{α} radiation (Rigaku Miniflex X-ray powder diffractometer, operated at 40 kV and scan rate was 2° min^{-1} with step of 0.02°). FTIR spectra were obtained by a Perkin-Elmer 2000-FTIR. KBr was mixed with a solid sample by an agate mortar and pestle to prepare a pellet specimen for identifying the samples. The specific surface areas of powders were measured by Brunauer-Emmett-Teller (BET) nitrogen gas absorption method. The powder microstructures were identified by scanning electron microscope (SEM, 145OVP LEO).

The dried samples were ground, sieved at 45 microns and uniaxially pressed (~ 30 Mpa) into pellet with 13 mm diameter, 1.5 mm thickness and subsequently isostatically pressed (CIP) at ~200 MPa. The dense pellets were prepared by stepwise sintering in air, at 700°C, 2 h, and at 1100°C, 2 h and naturally cooled in the furnace. The Archimedes was used to determined bulk density and X-ray diffraction analysis was carried out on the polished sintered ceramic pellet samples. Gold electrodes were painted on both faces of the pellets using gold paste and then fired at 800°C for 2 h. The dielectric constants (K) and dielectric loss factors (tan δ) of these pressed pellets were measured at room temperature between 1-1000 kHz using LCR meter (4194A, Hewlett Packard).

3. Results and discussion

3.1. Characterization of Metal-Organic Complex Precursors

Figure 2 comparatively shows the FTIR spectra of a free ligand, TEA and metal-organic complex precursor for preparing $LaFeO_3$ (LFO) ceramic. In the FTIR spectrum of La-Fe-TEA complex, Figure 2(b), the broad band located at around 3382 cm^{-1} was assigned for the stretching of O-H groups which is due to the moisture absorption and/or the TEA residue from the reaction. The very weak band around 2950-2870 cm^{-1} correlated with the absorption of C-H stretching vibration for $-CH_2-$ group and the peaks in the region of 1477-1325 cm^{-1} were assigned to the C-H bending. The band at 1640 cm^{-1} was attributed to O-H overtone. The small peaks at about 935 and 1074 cm^{-1} were ascribed to the C-O and C-N stretching, respectively. FTIR spectrum of metal-TEA complex (Figure 2(b)) exhibited a significant peaks shifted from that of free TEA ligand (Figure 2(a)). The strong bands of C-H stretching at about 2882 cm^{-1} and the sharp peaks of C-N at 1152 cm^{-1} and C-O stretching at 1035 cm^{-1} are obviously affected by the N and O coordinating atoms of TEA. In addition, the small absorption peak at 518 cm^{-1} is assigned to M-O or M-N stretching of metal coordinated with TEA ligand. Consequently, observation of the C-O and C-N stretching of coordinating ligand slightly shifted to lower frequencies, denoting the formation of metal-organic complex. FTIR spectra of the Co(II)-doped perovskite oxide precursors are similar to that of undoped LFO precursor.

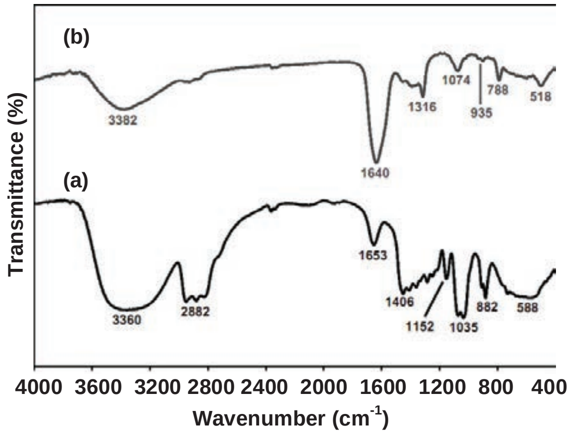

Fig. 2. FTIR Spectra of (a) Free Ligand, TEA and (b) Metal-organic Complex

Unfortunately, an attempt to recrystallize metal-organic complex precursors failed because of their high stability and undissolved in any solvent such as methanol, ethanol, acetone, hexane, acetonitrile, dichloromethane, ethyl acetate or chloroform. Thus, further characterizations and their structures could not be carried out.

To obtained ceramic powders, the prepared complexes were calcined to remove the organic contents. The calcination temperature and weight loss phenomena of complexes were determined by TGA.

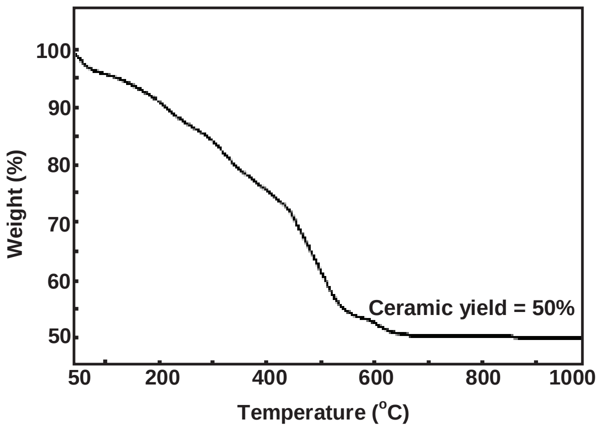

Fig. 3. TGA Thermogram of Metal-organic Complex Precursor

Figure 3 shows the TGA thermogram of undoped LFO precursor. There are three regions of weight loss. The first weight loss occurring below 200°C resulted from water evaporation and organic solvent decomposition. The second weight loss ranging from 200°C up to 500°C corresponded to oxidation of the organic contents, generating volatiles and char. Finally, the slight weight loss was found from 500°C to

700°C and it was ascribed to the burning of carbon-residue. Above 700°C, no weight loss was observed, showing that the appropriate temperature for calcining and converting the complexes to ceramic powders is started at 700°C.

Based on TGA result, all complexes were calcined at 850°C for 2 h to ensure that all of organic contents were completely removed.

3.2. Characterization of Ceramic Powders

Figures 4 (a) and (b) show XRD patterns of the as-prepared ceramic powders calcined at 850°C for 2 h, namely, $LaFeO_3$ (LFO), $La_{0.9}Co_{0.1}FeO_3$ (LCFO-1), $La_{0.8}Co_{0.2}FeO_3$ (LCFO-2), $La_{0.7}Co_{0.3}FeO_3$ (LCFO-3), $LaFe_{0.9}Co_{0.1}O_3$ (LFCO-1), $LaFe_{0.8}Co_{0.2}O_3$ (LFCO-2) and $LaFe_{0.7}Co_{0.3}O_3$ (LFCO-3). The XRD spectrum of each ceramic displayed the reflections corresponding to the orthorhombic structure of perovskite $LaFeO_3$ (JCPDS file no. 37-1493). However, as increasing amounts of Co(II) dopant, a small shift to higher 2-theta values of diffraction peaks was observed and trace impurity of CoO was also detected, indicating by the increasing of peaks intensity at 2-theta values of 36.6 and 74.0 degree for the LCFO and LFCO series, Figures 4 (a) and 4 (b), respectively. In addition, the diffraction peaks are a bit broaden as obviously seen in the LFCO series (Figure 4 (b), suggesting that the A site, La(III) or the B site, Fe(III) of $LaFeO_3$ perovskite was partly substituted by Co(II) so that no phase change in XRD was observed.

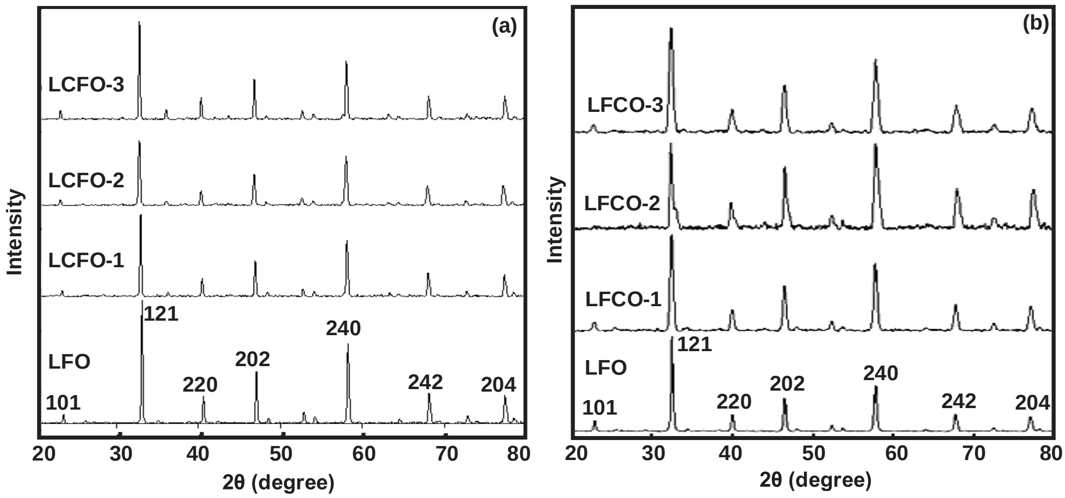

Fig. 4. XRD Patterns of the Obtained Products Calcined at 850°C for 2 h
(a) $La_{1-x}Co_xFeO_3$ (LCFO) and (b) $LaFe_{1-x}Co_xO_3$ (LFCO)

FTIR spectra show strong and sharp peak at 562-576 cm^{-1} which is attributed to antisymmetric stretching vibration of Fe-O in BO_6 octahedral unit of perovskite oxide ABO_3 as shown in Figure 5. A slight shift of Fe-O mode indicating that Fe-O bond strength was affected by Co(II) substitutution, similar to that reported in calcium-substituted $LaFeO_3$ [16]. As Co(II) has lower oxidation state than Fe(III), by substituton Co(II) to Fe(III) lattice site, in order to maintain the structure electroneutrality, oxygen vacancies are generated. Consequently, BO_6 octahedra in the perovskite structure were distorted. This might be responsible for the weakness of Fe-O bond stretching vibration and shift towards lower frequency with the increasing of Co(II) concentration. Moreover, the weak band at ~1500 cm^{-1} was observed. This ascribed to -COO wagging vibration of CO_3^{2-}, demonstrating that the sample contained certain amounts of impurity which occurred during thermal decomposition of metal-organic complex and could be destroyed if longer heat treatment is applied.

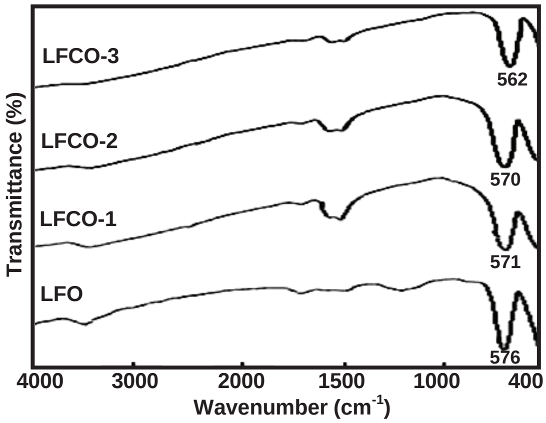

Fig. 5. FTIR Spectra of $LaFeO_3$ and $LaFe_{1-x}Co_xO_3$ Calcined at 850°C for 2 h

Surface area and porosity characteristics of the powders are illustrated in Table 1. BET surface area of LFO was 10.06 m^2/g which was higher than that prepared by other methods reported elsewhere [16-18]. The doped products, LCFO series illustrated relatively low specific areas of ~ 5 m^2/g while that of LFCO series varied in the range of 9.40-25.88 m^2/g. It is surprising that with increasing Co(II) content the BET surface area shows contrary tendency. The higher surface area in the LFCO series possibly due to increase in porosity.

Table 1. BET Surface Area, Porosity and Pore size of the Powders Calcined at 850°C for 2 h

Sample	Notation	BET surface area (m^2/g)	Pore volume (cm^3/g)	Pore size (nm)
$LaFeO_3$	LFO	10.06	0.03	12.79
$La_{0.9}Co_{0.1}FeO_3$	LCFO-1	5.98	0.01	5.77
$La_{0.8}Co_{0.2}FeO_3$	LCFO-2	5.69	0.01	6.39
$La_{0.7}Co_{0.3}FeO_3$	LCFO-3	5.25	0.01	5.90
$LaFe_{0.9}Co_{0.1}O_3$	LFCO-1	9.40	0.02	8.05
$LaFe_{0.8}Co_{0.2}O_3$	LFCO-2	19.34	0.02	4.85
$LaFe_{0.7}Co_{0.3}O_3$	LFCO-3	25.88	0.01	2.31

The SEM micrographs of some perovskite powders prepared are shown in Figure 6. The morphology of the LFO powder exhibited homogeneous and porous microstructure (Figure 6 (a)). Denser microstructure was observed in the LCFO-3 due to particle agglomerated (Figure 6 (b)), corresponding to lower specific areas of 5.25 m^2/g. Agglomeration in LFCO-3 exhibited irregular shape of block-like particles with homogeneous particles distribution and various size of porosity (Figure 6 (c)). This might be responsible for the highest surface area of 25.88 m^2/g found in LFCO-3.

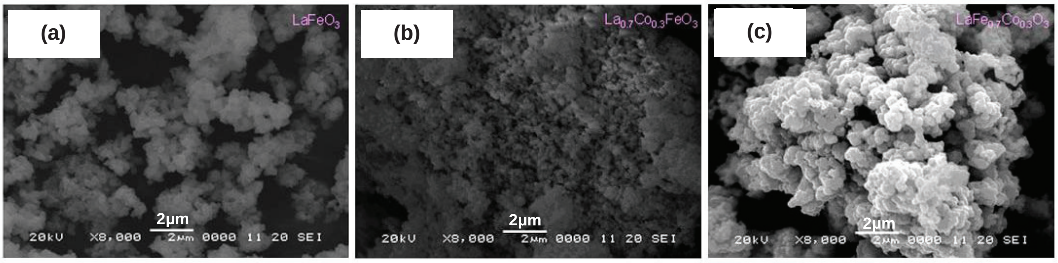

Fig. 6. SEM Micrographs of Ceramics Powder Calcined at 850°C for 2 h
(a) LFO, (b) LCFO-3 and (c) LFCO-3

3.3. Studied Dielectric Properties of Pellet Samples

3.3.1 Characterization of Pellets

Prior to dielectric measurement, density of pellet samples sintering at 1100°C for 2 h were determined. The density of all pellets was higher than 90% of theoretical density as presented in Table 2. The phase identification of pellet samples confirmed by XRD showed identical diffraction pattern as that of $LaFeO_3$ (Figures 7 (a) and (b)). It was found that diffraction peaks of each pellet became narrower and stronger, indicating a high degree of crystallinity.

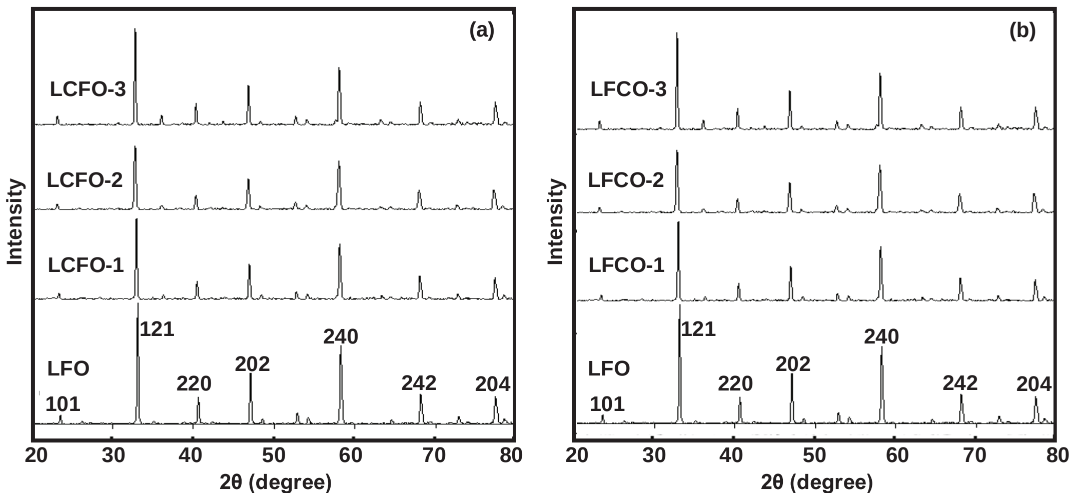

Fig. 7. XRD Patterns of the Sintering Pellet at 1100°C for 2 h (a) $La_{1-x}Co_xFeO_3$ (LCFO) and (b) $LaFe_{1-x}Co_xO_3$ (LFCO)

Figure 8 shows SEM micrograph of LCFO and LFCO pellet samples sintering at 1100°C for 2 h. For lowest concentration of Co(II) dopant, LCFO-1 and LFCO-1, smaller grains and grain boundary were obtained. With higher concentration of dopant, larger grain sizes and looser microstructures were observed, corresponding to lower density of pellet samples (Table 2).

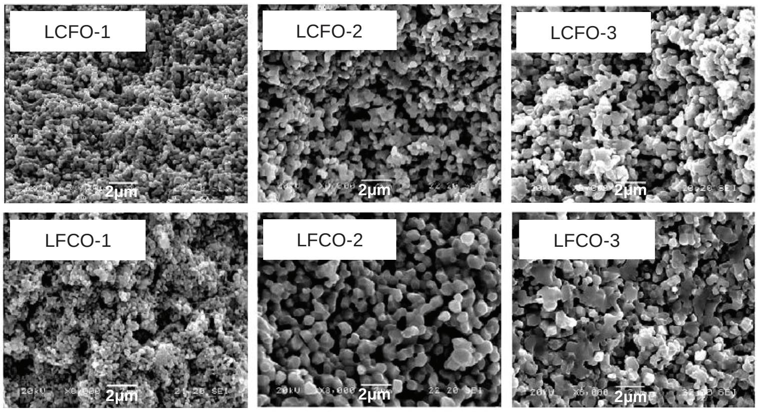

Fig. 8. SEM Micrograph of LCFO and LFCO Pellet Samples Sintering at 1100°C for 2 h

Table 2. Density (% of the Theoretical Density) of Pellets Samples Sintering at 1100°C for 2 h

Sample	Density (% theoretical)	Sample	Density (% theoretical)
LCFO-1	92	LFCO-1	98
LCFO-2	91	LFCO-2	97
LCFO-3	91	LFCO-3	91

3.3.2 Dielectric Behaviors of Co(II)-doped $LaFeO_3$ Pellets

Figures 9 and 10 demonstrate the variation of dielectric constant (K) and dielectric loss (tan δ) as a function of frequency measured at room temperature. With increasing frequency, all the pellets in LCFO and LFCO series exhibited dispersion and relaxation in dielectric constant and the dielectric constant found in LCFO series was much lower compared to that of LFCO series (Figure 9(A) and Figure 10(A)).

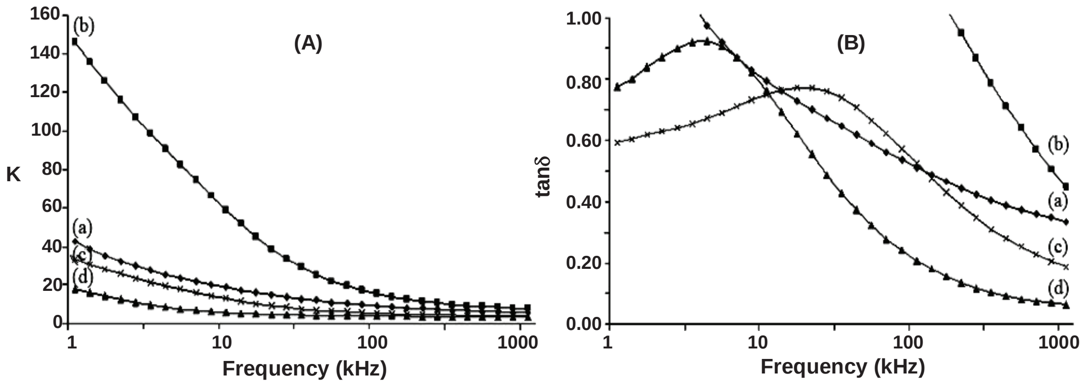

Fig. 9. Dielectric Constant, K (A) and Dielectric Loss Factor, tan δ (B) of $LaCo_xFe_{1-x}O_3$ vs Frequency at Room Temperature: (a) LFO, (b) LCFO-1, (c) LCFO-2 and (d) LCFO-3

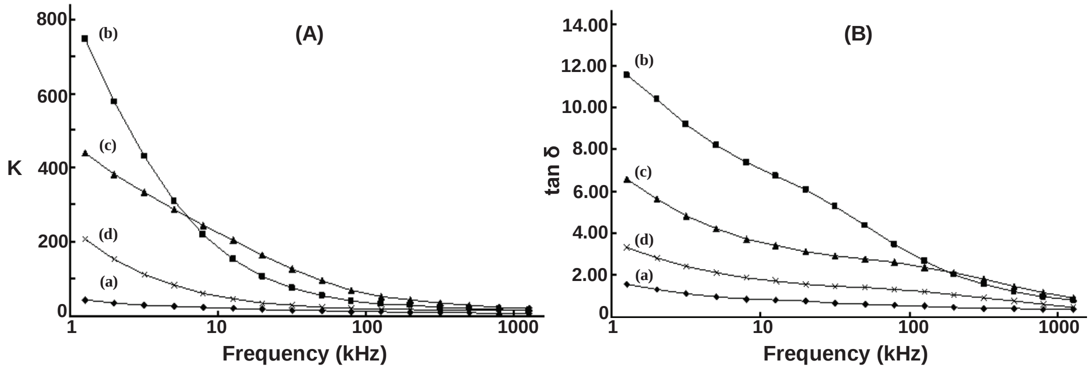

Fig. 10. Dielectric Constant, K (A) and Dielectric Loss Factor, tan δ (B) of $LaFe_{1-x}Co_xO_3$ vs Frequency at Room Temperature: (a) LFO, (b) LFCO-1, (c) LFCO-2 and (d) LFCO-3

In LCFO series, only dielectric constant of $La_{0.9}Co_{0.1}FeO_3$ (LCFO-1) was enhanced exhibiting dielectric constant of 150-10 between 1-1000 kHz (Figure 9(A)-(b)), however, its dielectric loss was higher than 0.5 over the same range (Figure 9(B) -(b)), suggesting that electrical behavior was dominated.

In LFCO series, the dielectric constants of all three compounds, LFCO-1, LFCO-2 and LFCO-3 were enhanced. As increasing the amount of Co(II) dopant, the dielectric constant decreased. The dielectric constant of $LaFe_{0.9}Co_{0.1}O_3$ (LFCO-1) is 750-13 (Figure 10(A)-(b)) and its dielectric loss is 12-0.8 (Figure 10(B)-(b)) over the frequency range of 1-1000 kHz. Because of the high dielectric losses of all the pellet samples in LFCO series, it indicated electrical behavior in all range of frequency (Figure 10(B)).The highest dielectric constant found in both Co(II) doping series, LCFO-1 and LFCO-1 might be associated to the smallest grains sizes and grain boundary as presented in Figure 8. Since few dielectric properties of the related $LaFeO_3$-based compounds have been studied, their dielectric properties have been unclear so far [15].

When Co(II) occupies the sites of La(III) or Fe(III) in the crystal lattice, in the view of charge compensation, oxygen vacancies are produced to maintain a neutral charge, consequently, holes are generated, resulting in non-stoichiometric $La_{1-x}Co_xFeO_{3-\delta}$ and $LaFe_{1-x}Co_xO_{3-\delta}$ compounds. As a result of holes producing in the structure of Co(II)-doping sample, the conductivity was enhanced resulting in high dielectric loss, showing low potential for use as dielectric materials. So that $La_{1-x}Co_xFeO_3$ and $LaFe_{1-x}Co_xO_3$ are one group of the modification $LaFeO_3$ p-type semiconductors that may be useful for gas sensing application.

4. Conclusion

$La_{1-x}Co_xFeO_3$ and $LaFe_{1-x}Co_xO_3$ (x = 0, 0.1, 0.2 and 0.3) powders were successfully prepared from metal-organic complex decomposition synthesized from the reaction of $LaNO_3.6H_2O$, $Fe(NO_3)_2.9H_2O$, triethanolamine ($N(CH_2CH_2OH)_3$) and appropriate amount of cobalt(II) chloride ($CoCl_2{\cdot}6H_2O$). XRD results showed that all the compounds were perovskite phase with orthorhombic structure. The specific surface areas of ceramics in LCFO series is ~ 5 m^2/g while that of LFCO series increased when the amount of Co(II) dopants increases and found in the range of 9.40- 25.88 m^2/g. From the investigation of the dielectric constant and dielectric loss, we found that $La_{1-x}Co_xFeO_3$ and $LaFe_{1-x}Co_xO_3$ showed p-type semiconducting properties. The dielectric loss of the $LaFeO_3$ increased with Co(II) doping, especially in $LaFe_{0.9}Co_{0.1}O_3$, corresponding to the increasing of electrical conductivity.

Acknowledgements

Financial supports of this work were provided by Faculty of Science, Kasetsart University and Kasetsart University Research and Development Institute (KURDI), Kasetsart University.

References

[1] Tai LW, Nasrallah MM, Anderson HU, Sparlin DM, Sehin SR. Structure and electrical properties of $La_{1-x}Sr_xCo_{1-y}Fe_yO_3$. Part 2. The system $La_{1-x}Sr_xCo_{0.2}Fe_{0.8}O_3$. *Solid State Ionics* 1995;**76**:273–83.

[2] Bidrawn F, Kim G, Aramrueang N, Vohs JM, Gorte RJ. Dopants to enhance SOFC cathodes based on Sr-doped $LaFeO_3$ and $LaMnO_3$. *J Power Sources* 2010;**195**:720–28.

[3] Murata K, Fukui T, Abe H, Naito M, Nogi K.. Morphology control of $La(Sr)Fe(Co)O_{3-a}$ cathodes for IT-SOFCs. *J Power Sources* 2005;**145**:257–61.

[4] Takeda Y, Kanno R, Noda M, Tomida Y, Yamamoto O. Cathodic Polarization Phenomena of Perovskite Oxide Electrodes with Stabilized Zirconia. *J Electrochem Soc* 1987;134:2656–661.

[5] Li KY, Wang DJ, Wu FQ, Li TF. Surface electronic states and photovoltage gas-sensitive characters of nanocrystalline $LaFeO_3$. *Mater Chem Phys* 2000;**64**:269–72.

[6] Song, P.; Hu, J.; Qin, H.; Zhang, L.; An, K. Preparation and ethanol sensitivity of nanocrystalline $La_{0.7}Pb_{0.3}FeO_3$-based gas sensor. *Mater Lett* 2004;**58**:2610–13.

[7] Song P, Qin H, Zhang L, An K, Lin Z, Hu J, Jiang M. The structure, electrical and ethanol-sensing properties of $La_{1-x}Pb_xFeO_3$ perovskite ceramics with $x\leq0.3$. *Sens Actuators, B* 2005;**104**:312–16.

[8] Toan NN, Saukko S, Lantto V. Gas sensing with semiconducting perovskite oxide $LaFeO_3$. *Physica B* 2003;**327**:279–82.

[9] Świerczek K, Dabrowski B, Suescun L, Kolesnik S. Crystal structure and magnetic properties of high-oxygen pressure annealed $Sr_{1-x}La_xCo_{0.5}Fe_{0.5}O_{3-\delta}$ ($0\leq x\leq0.5$). *J Solid State Chem* 2009;**182**:280–88.

[10] Li K, Wang D, Wu F, Xie T, Li T. Surface electronic states and photovoltage gas-sensitive characters of nanocrystalline LaFeO3. *Mater. Chem. Phys*. 2000;**64**:269–72.

[11] Qi XW, Zhou J, Yue ZX, Gui ZL, Li LT. A simple way to prepare nanosized $LaFeO_3$ powders at room temperature. Ceram Int 2003;**29**:347–49.

[12] Xiao J, Hong GY, Yu DC, Dong XT. Synthesis and properties of $LaFeO_3$ ultrafine powders. *Acta Chim. Sinica* 1994;**52**:784–88.

[13] Li S, Jing L, Fu W, Yang L, Xin B, Fu H. Photoinduced charge property of nanosized perovskite-type $LaFeO_3$ and its relationships with photocatalytic activity under visible irradiation. *Mater Res Bull* 2007;**42**:203–12.

[14] Vidyasagar K, Gopalakrishan J, Rao CNR. Synthesis of complex metal oxides using hydroxide, cyanide, and nitrate solid solution precursors. *J Solid State Chem* 1985;**58**:29–37.

[15] Komine S, Iguchi E. Dielectric properties in $LaFe_{0.5}Ga_{0.5}O_3$. *J Phys Chem Solids* 2007;**68**:1504–507.

[16] Barbero B P, Gamboa JA, Cadús LE. Synthesis and characterisation of $La_{1-x}Ca_xFeO_3$ perovskite-type oxide catalysts for total oxidation of volatile organic compounds. *Appl Catal, B* 2006;**65**:21–30.

[17] Nakayama S. $LaFeO_3$ perovskite-type oxide prepared by oxide-mixing, co-precipitation and complex synthesis methods. *J Mater Sci* 2001;**36**:5643–48.

[18] Wang Y, Zhu J, Zhang L, Yang X, Lu L, Wang X. Preparation and characterization of perovskite $LaFeO_3$ nanocrystals. *Mater Lett* 2006;**60**:1767–770.